JOURNAL OF Materials CHEMISTRY

Control of the size of platinum particles on silica surfaces using organic–inorganic composites

Kazuaki Ishii,[a] Fujio Mizukami,*[b] Hiroyuki Izutsu,[c] Fumi Taniguchi,[b] Yoshimichi Kiyozumi,[b] Kazuyuki Maeda[b] and Yuki Fujii[a]

[a]*Graduate School of Science and Engineering, Ibaraki University, Mito, Ibaraki 310-8512, Japan*
[b]*National Institute of Materials and Chemical Research, Tsukuba, Ibaraki 305-8565, Japan*
[c]*Taki Chemical Co., Ltd, Midorimachi, Befu-cho, Kakogawa, Hyogo 675-0124, Japan*

Received 5th October 1998, Accepted 8th February 1999

A series of two tartaric acid–silica (sol–gel and impreg tart-SiO_2) composites with different tartaric acid contents were prepared using sol–gel and impregnation methods, and then a series of two platinum–silica composites (impreg·sol–gel Pt-SiO_2 and impreg·impreg Pt-SiO_2) were obtained by impregnating sol–gel and impreg tart-SiO_2 with a platinum solution, followed by drying and calcining. The platinum–silica composites which were obtained were characterized by XRD, N_2 and H_2 adsorption and SEM. From the results, it is concluded that the distribution and particle size of platinum in Pt-SiO_2 can be controlled by using two types of tartaric acid–silica composites with different tartaric acid contents, while keeping the platinum loading constant.

Introduction

Tailoring inorganic solid surfaces is of great importance in fields such as catalysis, separation, and chemical sensing. Recently, it has been shown that organic–inorganic interfaces can play an important role in oriented nucleation, crystal morphology,[1–7] and the formation of size-controlled pores[7–12] and particles[5–7,13] of inorganic materials, as well as providing a new method for the fabrication of inorganic materials. We have already shown that the structure,[14–16] particle size,[17] pore size[18,19] and surface area[20] of metal oxides can be controlled by using certain organic polydentate ligands in the sol–gel process. Here we report control of the distribution and dispersion of the metal in metal-loaded oxides, using two types of organic composites in which the distribution and dispersion of the organic compounds differ. We also provide details of the unique discovery of the appearance of rings of small metal particles.

Experimental

Preparation of catalysts

All chemicals were guaranteed reagent grade, unless otherwise stated.

Impreg·sol–gel Pt-SiO_2 series. Tetraethoxysilane (0.3 mol) was mixed with L-tartaric acid (tart; 0.025–0.3 mol) in isopropanol (0.83 mol) in the presence of acetic acid (0.1 mol) at 353 K for 2 h. Water (0.6 mol) was then added and the resultant viscous solution was aged overnight at the same temperature before being dried at 353 K *in vacuo* and subsequently ground to a powder (sol–gel tart-SiO_2). The powder was evacuated at 353 K, impregnated with an acetone solution of $H_2PtCl_6{\cdot}6H_2O$ at ambient temperature, stirred for several hours, then dried at 298 K *in vacuo*. Finally, the Pt-impregnated powder (impreg·sol–gel Pt-tart-SiO_2) was calcined at 723 K for 2 h and reduced in an atmosphere of hydrogen at 573 K for 2 h to give the impreg·sol–gel Pt-SiO_2.

Impreg·impreg Pt-SiO_2 series. The silica was first prepared by the hydrolysis of tetraethoxysilane and calcined at 573 K for 3 h. The ethanol solution of tartaric acid was then impregnated onto the silica (impreg tart-SiO_2). After solvent removal and drying, the acetone solution of $H_2PtCl_6{\cdot}6H_2O$ was impregnated onto the dry powder, impregnated with tartaric acid, followed by drying (impreg·impreg Pt-tart-SiO_2), calcination and reduction (impreg·impreg Pt-SiO_2), as described previously.

The platinum content was 5 wt% ($Pt/SiO_2 = 0.016$) in all Pt-SiO_2 samples.

Measurements

The X-ray powder diffraction patterns were obtained on a MAC Science MXP-18 (MAC Science, Tokyo, Japan) instrument using Cu-Kα radiation with a Ni filter. The size of platinum particles was determined from the reflection (d= 2.265 Å, 111) of platinum metal using the Scherrer equation. Some of the XRD patterns used for determining the platinum particle size are shown in Fig. 3 (later). Specific surface area was determined by the BET method from nitrogen adsorption data at 77 K, using a BELSORP 36 (BEL Japan, Osaka, Japan). The pore-size distribution was calculated by the Horvath–Kawazoe method from nitrogen adsorption data. H_2 chemisorption on the catalysts was carried out at 273 K after evacuating the system to 10^{-4} Pa at 673 K for 3 h using a BELSORP 36 (BEL Japan, Osaka, Japan). The SEM images were obtained using a Hitachi S-800 (Hitachi, Tokyo, Japan). Thermogravimetry and differential thermal analyses were carried out on a MAC science TG-DTA 2000 (MAC Science, Tokyo, Japan) instrument with a heating rate of 10 K min^{-1} under a flow of 100 cm^3 min^{-1} of dry nitrogen.

Results

The dispersion of tartaric acid and platinum in the catalysts

X-Ray diffraction patterns of tart-SiO_2, Pt-tart-SiO_2, and Pt-SiO_2 are shown in Fig. 1. All Pt-SiO_2 samples prepared here showed the crystalline phase of the platinum metal (a6, a7, b6 and b7 in Fig. 1), independent of the tart/SiO_2 ratios of the tart-SiO_2 composites and the preparation procedure.

For the tart-SiO_2 samples, all impreg tart-SiO_2 composites showed XRD patterns characteristic of tartaric acid crystals; the XRD reflections were very sharp. However, the sol–gel tart-SiO_2 composites with tart/$SiO_2 \leqslant 0.83$ gave no clear reflections, and the composites with tart/$SiO_2 = 1.0$ showed only weak reflections, indicating the existence of small tartaric acid crystals.

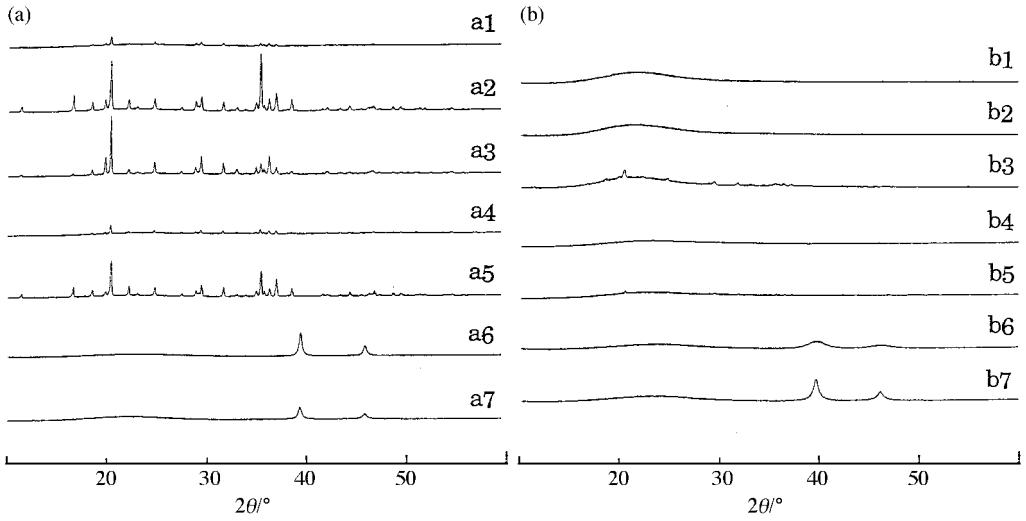

Fig. 1 XRD patterns of tart-SiO_2, Pt-tart-SiO_2, and Pt-SiO_2. Impreg·impreg series (a): a_1, tart-SiO_2 (tart/SiO_2 = 0.27); a_2, tart-SiO_2 (tart/SiO_2 = 0.60); a_3, tart-SiO_2 (tart/SiO_2 = 0.93); a_4, Pt-tart-SiO_2 (tart/SiO_2 = 0.27); a_5, Pt-tart-SiO_2 (tart/SiO_2 = 0.60); a_6, Pt-SiO_2 (tart/SiO_2 = 0.27); a_7, Pt-SiO_2 (tart/SiO_2 = 0.97). Impreg·sol–gel series (b): b_1, tart-SiO_2 (tart/SiO_2 = 0.33); b_2, tart-SiO_2 (tart/SiO_2 = 0.66); b_3, tart-SiO_2 (tart/SiO_2 = 1.0); b_4, Pt-tart-SiO_2 (tart/SiO_2 = 0.25); b_5, Pt-tart-SiO_2 (tart/SiO_2 = 0.50); b_6, Pt-SiO_2 (tart/SiO_2 = 0.25); b_7, Pt-SiO_2 (tart/SiO_2 = 1.0).

All impreg·impreg Pt-tart-SiO_2 composites prepared here displayed XRD patterns characteristic of tartaric acid crystals. Some impreg·sol–gel Pt-tart-SiO_2 composites with higher tartaric acid contents (here b5) also showed very weak XRD reflections, owing to the presence of tartaric acid crystals; however, this was because a small amount of tartaric acid, which was dissolved out of the composites into the solvent on impregnating with a platinum solution, was crystallized onto the silica surface by the evaporation of the solvent, because sol–gel tart-SiO_2 composites, with tart/$SiO_2 \leqslant 0.83$, showed no clear XRD reflections.

TG and DTA profiles of two series of tart-SiO_2 and Pt-tart-SiO_2 are given in Fig. 2 and 3. Each impreg tart-SiO_2 sample showed a very sharp endothermic peak without weight loss in the region of 443 K (melting point of L-tartaric acid) to 453 K,

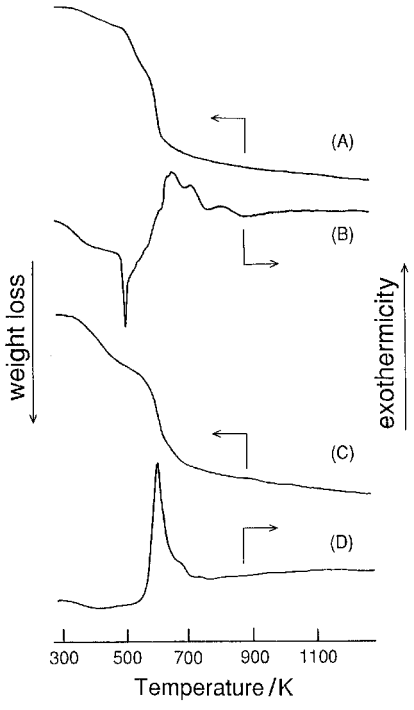

Fig. 2 Thermogravimetric analyses and differential thermal analyses of two series of tart-SiO_2. Impreg tart-SiO_2 (tart/SiO_2 = 0.93): (A) TG; (B) DTA. Sol–gel tart-SiO_2 (tart/SiO_2 = 0.83): (C) TG; (D) DTA.

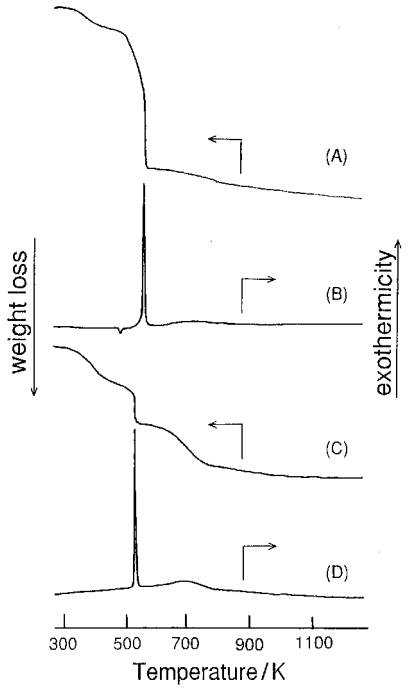

Fig. 3 Thermogravimetric analyses and differential thermal analyses of two series of Pt-tart-SiO_2. Impreg·impreg Pt-tart-SiO_2 (tart/SiO_2 = 0.17): (A) TG; (B) DTA. Impreg·sol–gel Pt-tart-SiO_2 (tart/SiO_2 = 0.33): (C) TG; (D) DTA.

and the peak height increased with increasing tartaric acid content. However, the sol–gel tart-SiO_2 composites, with tart/$SiO_2 \leqslant 0.83$, showed no such peak, and the composite with tart/SiO_2 = 1.0 showed a very broad, weak endothermic peak. These results indicate that in samples prepared by the sol–gel procedure, tartaric acid molecules did not form aggregates, and were highly dispersed throughout the composites, whereas in the impregnation procedure, the molecules formed ordered aggregates. In addition, after impregnation with platinum, the weight loss (occurring at 453–633 K before the impregnation), arising from the decomposition and combustion of tartaric acid, shifted to slightly higher temperatures and split into two distinct loss steps, corresponding to two types of tartaric acid: coordinated and not coordinated to platinum. On the other hand, it was difficult to identify Pt-tart complexes in the

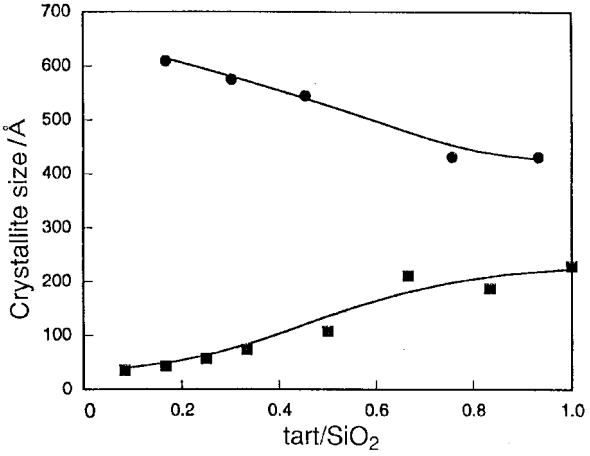

Fig. 4 Effect of the tart/SiO_2 ratio on the size of platinum particles in Pt-SiO_2 prepared *via* tart-SiO_2. ■, Impreg·sol–gel Pt-SiO_2; ●, Impreg·impreg Pt-SiO_2.

composites from the NMR and IR spectra because of strong signals resulting from a large amount of uncoordinated tartaric acid.

Platinum metal particle size and H_2 chemisorption

Fig. 4 shows the effect of the tart/SiO_2 ratio on platinum particle size for the Pt-SiO_2 samples prepared *via* two series of tart-SiO_2 composites. The X-ray diffraction results for the Pt-SiO_2 samples suggest a relationship between the tartaric acid content and the platinum particle size: namely, for the impreg·sol–gel Pt-tart-SiO_2 samples the platinum particle size increased as the tartaric acid content increased, until reaching an almost constant value. In contrast, for the impreg·impreg Pt-tart-SiO_2 samples the platinum particle size decreased as the tartaric acid content increased, before reaching a constant value.

Table 1 shows the results of H_2 chemisorption. It is well documented that the amount of adsorbed hydrogen increases as the loaded metal becomes highly dispersed, in other words, as the size of the metal particles becomes small. For the impreg·sol–gel Pt-SiO_2 series, the amount of adsorbed hydrogen increased as the tart/SiO_2 ratio decreased, indicating a relationship between the amount of adsorbed hydrogen and the platinum particle size in Pt-SiO_2: namely, the Pt-SiO_2 which had a smaller platinum particle size, as shown in Fig. 4, adsorbed a greater amount of hydrogen. On the other hand, for the impreg·impreg Pt-SiO_2 series, which had a larger platinum particle size compared with those of the impreg·sol–gel Pt-SiO_2 samples, the change in the amount of adsorbed hydrogen between samples was small, and it was difficult to find a dependence of the adsorbed amount on the tart/SiO_2 ratio.

Specific surface area and pore distribution

Table 2 shows the specific surface areas, as determined by the BET method, from nitrogen adsorption data of Pt-SiO_2. For

Table 1 Hydrogen chemisorption of Pt-SiO_2

Preparation method	tart/SiO_2	H_2 chemisorption (H_2 mol/Pt mol)
Sol–gel·impreg	0.17	6.63×10^{-1}
	0.50	2.93×10^{-1}
	0.83	2.66×10^{-1}
Impreg·impreg	0.17	1.97×10^{-1}
	0.46	2.01×10^{-1}
	0.76	1.50×10^{-1}

Table 2 Specific surface area of Pt-SiO_2

Sol–gel·impreg		Impreg·impreg	
tart/SiO_2	surface area/$m^2\ g^{-1}$	tart/SiO_2	surface area/$m^2\ g^{-1}$
0.08	650		
0.17	688	0.17	232
0.25	732	0.30	203
0.33	789	0.46	192
0.50	869	0.75	124
0.67	965	0.93	79
0.83	982		

the impreg·sol–gel Pt-SiO_2, the surface area increased from 650 to 980 $m^2\ g^{-1}$ as the tart/SiO_2 ratio increased. We have already reported that the specific surface area of silica, prepared by the sol–gel method using tartaric acid, can be changed (600–1200 $m^2\ g^{-1}$),[21,22] so this phenomenon can be explained from the effect of the tartaric acid on the hydrolysis and the formation of pores caused by the tartaric acid remaining in a gel. Thus, it is found that the particle size of platinum increases with an increase in the surface area of the silica support, in spite of the constant platinum content. With regard to the impreg·impreg Pt-SiO_2 series, no large change in the specific surface area, compared with those of the impreg·sol–gel Pt-SiO_2 series, was observed because the same calcined silica was used as the support (specific surface area: 320 $m^2\ g^{-1}$). However, the surface area slightly decreased as the tartaric acid content increased, indicating that the decrease in the surface area was induced by the sintering of silica caused by the decomposition and combustion of tartaric acid during the heat treatment. In this case, in contrast to the above impreg·sol–gel series, the particle size of platinum decreased with a decrease in the silica surface area. Anyhow, it should be noticed that these relationships between the platinum particle size and the surface area of silica were opposite to those expected generally, because the particles of the supported metal were considered to become smaller in size as the surface area of the support increased.

Fig. 5 shows the pore distributions of the impreg·sol–gel Pt-SiO_2, determined by the Horvath–Kawazoe method. The Pt-SiO_2 composites with tart/SiO_2 = 0.08 displayed a broad distribution, ranging between 2 and 5 nm. The pore diameter decreased and the pore distributions became very sharp as the ratio of tart/SiO_2 increased. Also uniform pores around 2 nm in diameter were observed in the Pt-SiO_2 composites with tart/SiO_2 = 0.83. Conversely, in the impreg·impreg Pt-SiO_2 composites the pore distribution did not show such a clear peak, ranging instead from 1 to 100 nm; additionally, none of the silica used as the support had mesopores. Thus, in the impreg·sol–gel Pt-SiO_2 samples the silica particle size decreased

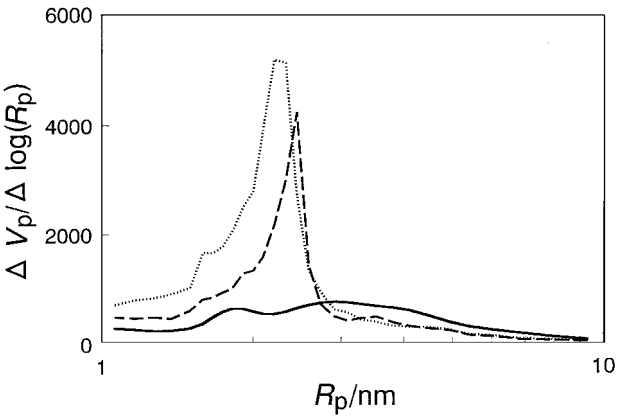

Fig. 5 Pore distributions of impreg·sol–gel Pt-SiO_2: (—) tart/SiO_2 = 0.08, (– – –) tart/SiO_2 = 0.33, (…) tart/SiO_2 = 0.83.

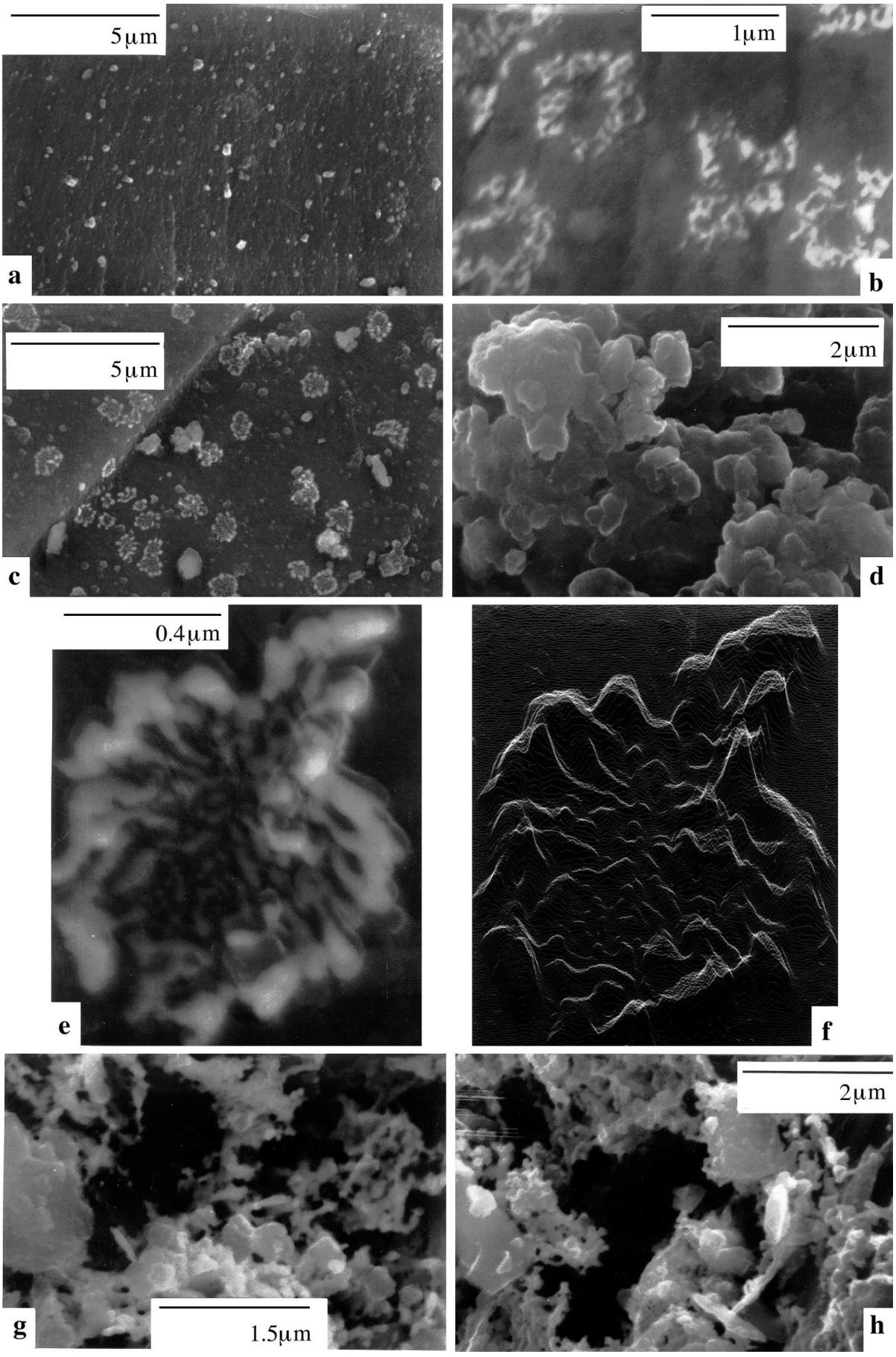

Fig. 6 SEM images of impreg·sol–gel Pt-SiO_2 (a–f) prepared from sol–gel tart-SiO_2 *via* impreg·sol–gel Pt-tart-SiO_2 and impreg·impreg Pt-tart-SiO_2 (g, h) prepared from impreg tart-SiO_2 *via* impreg·impreg Pt-tart-SiO_2. (a) tart/SiO_2 = 0.33; (b) tart/SiO_2 = 0.50; (c) tart/SiO_2 = 0.83; (d) tart/SiO_2 = 1.0; (e) magnification of one of the rings of dots in (c), which seem to have come out of the inside of the silica; (f) topographic image of (e); (g) tart/SiO_2 = 0.22; (h) tart/SiO_2 = 0.61.

as the tartaric acid content increased. The pore diameter also decreased. In the impreg·impreg Pt-SiO_2 samples, the pore diameter was independent of the tartaric acid content, similar to that of the silica support itself, and thus the surface area could be attributed to the size of the primary particles constituting the support and less than 1 nm in the particles.

SEM observations

As shown in Fig. 6, in the micrographs of impreg·sol–gel Pt-SiO_2 samples obtained from sol–gel tart-SiO_2 composites (tart/SiO_2 = 0.083 to 0.33) *via* impreg·sol–gel Pt-tart-SiO_2 composites, it was difficult to confirm the existence of platinum; however, the electron diffraction (EDX) mapping analysis revealed that platinum was finely and uniformly dispersed in the silica. When the tart/SiO_2 ratio was 0.5–0.83, the platinum appeared as rings of dots, or hillocks, and for tart/$SiO_2 \geqslant 0.83$, as a diffuse cloud or fog. For impreg·impreg Pt-SiO_2 samples prepared from impreg tart-SiO_2 composites *via* impreg·impreg Pt-tart-SiO_2, however, the platinum always appeared as a diffuse cloud or fog, whatever the tart/SiO_2 ratio.

The difference in the dispersion and distribution of platinum between the two series could be attributed to the difference in the dispersion and distribution of tartaric acid between the two series of Pt-tart-SiO_2 composites as stated below.

Discussion

Tartaric acid has two carboxy and two hydroxy groups, and strongly coordinates to metal ions. In the Pt-tart-SiO_2 composites, because more tartaric acid was present than platinum (tart/Pt = 5.2 to 63), most platinum ions will be coordinated by tartaric acid molecules. Based on this assumption and the XRD and TG-DTA results, the platinum and tartaric acid in Pt-tart-SiO_2 composites can be illustrated as in Fig. 7. In impreg tart-SiO_2 composites, the tartaric acid was dispersed on the silica surfaces as ordered aggregates or crystals. Accordingly, with a constant platinum content, as the tartaric acid content in the composites increased, initially the aggregates became larger, and the distances between platinum ions in the impreg·impreg Pt-tart-SiO_2 composite increased, until the whole surface of the silica support was fully covered with tartaric acid. This explains the effect of the tartaric acid content on the platinum particle size in the impreg·impreg Pt-SiO_2 series. Moreover, the appearance of platinum as a diffuse cloud or fog on the silica surface can be described as arising from a spray of tartaric acid during decomposition by the heat treatment.

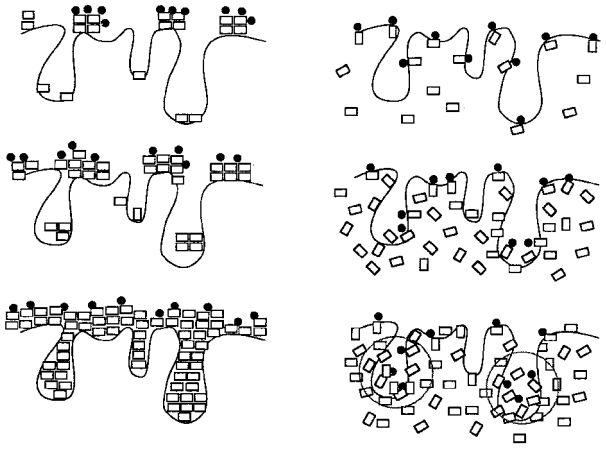

Fig. 7 Possible structures of Pt-tart-SiO_2. (Left) Impreg·impreg series. (Right) Impreg·sol–gel series. Platinum ions and tartaric acid are represented by ● and □, respectively. A circle means that the spinodal phase separation occurs easily.

For the impreg·sol–gel Pt-tart-SiO_2 composites, because tartaric acid was connected to the silicon of tetraethoxysilane by a substitution reaction, when sol–gel tart-SiO_2 composites were first prepared from tetraethoxysilane and tartaric acid, it was apt to remain in the silica networks on hydrolysis of the silanes, and must have existed as a disordered dispersion at the single-molecule level. However, tartaric acid molecules moved nearer to each other and tended to aggregate as the tartaric acid content increased. As larger tartaric acid aggregates could accommodate more platinum ions, the particle size of platinum in the impreg·sol–gel Pt-SiO_2 obtained by heat treatment of the impreg·sol–gel Pt-tart-SiO_2 composites became larger as the tartaric acid content in the composite increased. Additionally, the tartaric acid in the sol–gel tart-SiO_2 and impreg·sol–gel Pt-tart-SiO_2 composites seemed to result from a phase separation when the tartaric acid content in the composites was high. Because the miscibility between tartaric acid and silica decreased as the tartaric acid content increased (because tartaric acid is organic and silica is inorganic), the composites were apt to separate into tartaric acid and silica aggregates by thermal stress, for example. This separation is called spinodal decomposition, and has been observed in organic–silica composites.[23] In spinodal decomposition, a component in a metastable single phase diffuses against the concentration gradient to form masses, separated in the form of hillocks, by means of a nucleation-growth process. Such a phase separation occurs only in a special concentration range.[24–26] This characteristic was indeed shown in the scanning electron microscopy (SEM) images of impreg·sol–gel Pt-SiO_2 [Fig. 6(f)]. We deduce that the rings of Pt dots appeared on the silica surface as a result of spinodal phase separation of impreg·sol–gel Pt-tart-SiO_2 composites, caused by heat treatment.

Conclusions

From the results, it is concluded that the distribution and particle size of platinum in Pt-SiO_2 can be effectively controlled by using two types of tartaric acid–silica composites with different tartaric acid contents, while keeping the platinum loading constant.

Acknowledgement

We would like to express our thanks to Dr. Mark J. Jeffery for valuable discussions.

References

1 E. M. Landau, S. Grayer Wolf, M. Levanon, L. Leiserowitz, M. Lahav and J. Sagiv, *J. Am. Chem. Soc.*, 1989, **111**, 1436.
2 B. R. Heywood and S. Mann, *Adv. Mater.*, 1992, **4**, 278.
3 D. D. Archibald and S. Mann, *Nature*, 1993, **364**, 430.
4 J. M. Didymus, P. Oliver, S. Mann, A. L. DeVries, P. V. Hauschka and P. Westbroek, *J. Chem. Soc., Faraday Trans.*, 1993, **89**, 2891.
5 S. Mann, *Nature*, 1993, **365**, 499.
6 S. Mann, *J. Chem. Soc., Dalton Trans.*, 1993, 1.
7 S. Mann, D. D. Archibald, J. M. Didymus, T. Douglas, B. R. Heywood, F. C. Meldrum and N. J. Reeves, *Science*, 1993, **261**, 1286.
8 M. E. Davis, *Nature*, 1993, **364**, 391.
9 C. T. Kresge, M. E. Leonowicz, W. J. Roth, J. C. Vartuli and J. S. Beck, *Nature*, 1992, **359**, 710.
10 J. S. Beck, J. C. Vartuli, W. J. Roth, M. E. Leonowicz, C. T. Kresge, K. D. Schmitt, C. T. W. Chu, D. H. Olson, E. W. Sheppard, S. B. McCullen, J. B. Higgins and J. L. Schlenker, *J. Am. Chem. Soc.*, 1992, **114**, 10834.
11 A. Monnier, F. Schuth, Q. Huo, D. Kumar, D. Margolese, R. S. Maxwell, G. D. Stucky, M. Krishnamurty, P. Petroff, A. Firouzi, M. Janicke and B. F. Chmelka, *Science*, 1993, **261**, 1299.
12 Q. Huo, D. I. Margolese, U. Ciesla, P. Feng, T. E. Gier, P. Sieger,

R. Leon, P. M. Petroff, F. Schuth and G. D. Stucky, *Nature*, 1994, **368**, 317.
13 F. C. Meldrum, V. J. Wade, D. L. Nimmo, B. R. Heywood and S. Mann, *Nature*, 1991, **349**, 684.
14 F. Mizukami, Y. Kobayashi, S. Niwa, M. Toba and K. Shimizu, *J. Chem. Soc.*, *Chem. Commun.*, 1988, 1540.
15 K. Maeda, F. Mizukami, S. Miyashita, S. Niwa and M. Toba, *J. Chem. Soc.*, *Chem. Commun.*, 1990, 1268.
16 K. Kojima, F. Mizukami, M. Miyazaki and K. Maeda, *J. Non-Cryst. Solids*, 1992, **147 & 148**, 442.
17 F. Mizukami, S. Niwa, S. Ohkawa and A. Katayama, *Stud. Surf. Sci. Catal.*, 1993, **78**, 337.
18 K. Maeda, F. Mizukami, M. Watanabe, S. Niwa and M. Toba, *Chem. Ind.* (*London*), 1989, 807.
19 M. Toba, F. Mizukami, S. Niwa and K. Maeda, *J. Chem. Soc.*, *Chem. Commun.*, 1990, 1211.
20 S. Niwa, F. Mizukami, S. Isoyama, T. Tsuchiya, K. Shimizu, S. Imai and J. Imamura, *J. Chem. Technol. Biotechnol.,* 1986, **36**, 236.
21 H. Izutsu, F. Mizukami, Y. Kiyozumi and K. Maeda, *J. Am. Ceram. Soc.*, 1997, **80**, 2581.
22 F. Mizukami, H. Izutsu and T. Osaka, *Adv. Mater.*, 1994, **6**, 854.
23 K. Nakanishi and N. Soga, *J. Am. Ceram. Soc.*, 1991, **74**, 2518.
24 J. W. Cahn, *J. Chem. Phys.*, 1965, **42**, 93.
25 J. J. Hammel, *J. Chem. Phys.*, 1967, **46**, 2234.
26 J. W. Cahn, *Trans. Metall. Soc. AIME,* 1968, **242**, 166.

Paper 8/07703G